tvst

Article

Longitudinal Changes of Macular Curvature in Patients with Retinitis Pigmentosa

Monika Meinert[1,2], Shinji Ueno[1], Shiori Komori[1], Yoshito Koyanagi[1,3], Akira Sayo[1], Sten Andreasson[2], Taro Kominami[1], Yasuki Ito[1], and Hiroko Terasaki[1]

[1] Department of Ophthalmology, Nagoya University Graduate School of Medicine, Showa-ku, Nagoya, Japan
[2] Department of Ophthalmology, University of Lund, Lund, Sweden
[3] Department of Ophthalmology, Graduate School of Medical Sciences, Kyushu University, Nishi-ku, Fukuoka, Japan

Correspondence: Shinji Ueno, Department of Ophthalmology, Nagoya University Graduate School of Medicine, 65 Tsuruma-cho, Showa-ku, Nagoya 466-8550, Japan. e-mail: ueno@med.nagoya-u.ac.jp

Received: November 5, 2019
Accepted: August 3, 2020
Published: September 10, 2020

Keywords: retinitis pigmentosa; retinal photoreceptor layer; ellipsoid zone; macular curvature; spectral domain optical coherence

Citation: Meinert M, Ueno S, Komori S, Koyanagi Y, Sayo A, Andreasson S, Kominami T, Ito Y, Terasaki H. Longitudinal changes of macular curvature in patients with retinitis pigmentosa. Trans Vis Sci Tech. 2020;9(10):11, https://doi.org/10.1167/tvst.9.10.11

Purpose: To investigate the longitudinal changes of the macular curvature in eyes with retinitis pigmentosa (RP) and to determine the factors associated with the changes.

Methods: We reviewed the medical charts of 107 RP patients, for whom the axial length of their right eyes ranged from 21.5 to 26.0 mm and who had had been followed by spectral-domain optical coherence tomography (OCT). The OCT images at the initial and the most recent examinations were compared. The mean curvature of Bruch's membrane within 6 mm of the central macula obtained from the OCT images was evaluated as the mean macular curvature index (MMCI). Changes in the MMCI and their relationships with other clinical factors, including the ellipsoid zone (EZ) width, were assessed.

Results: The MMCI decreased significantly in the vertical OCT images, from -15.47×10^{-5} μm^{-1} to -16.36×10^{-5} μm^{-1} ($P = 0.008$) during the mean observation period of 3.4 ± 1.4 years (mean ± SD). This indicated that the macular shape became more concave. The change to a steeper shape was more prominent in eyes with less photoreceptor degeneration and for which the EZ width was preserved at >2000 μm. In three eyes, the MMCI increased markedly by $>5 \times 10^{-5}$ μm^{-1}, and this was accompanied by absorption of the macular edema.

Conclusions: The macular curvature in RP eyes becomes more concave in eyes with preserved EZ width.

Translational Relevance: Longitudinal changes of the macular curvature in RP should be considered in future therapies, such as the implantation of the retinal prosthesis.

Introduction

Retinitis pigmentosa (RP) is a heterogeneous group of inherited retinal disorders with degeneration of the rod and cone photoreceptors. The signs and symptoms of RP are impaired night vision, slow progressive peripheral-to-central visual field loss, and an eventual decline of visual acuity. Recent advancements in optical coherence tomography (OCT) have enabled clinicians to assess the anatomical alterations in different retinal disorders, and extensive studies have been performed to evaluate photoreceptor microstructures, such as the ellipsoid zone (EZ) and outer nuclear layer (ONL) in eyes with RP.[1–4] Analyses have shown that retinal degeneration can not only change the morphology of the neurosensory retina but also alter the shape of the posterior pole. In addition, there are some RP eyes in which a posterior staphyloma can be detected in the OCT images.[5–7] A staphyloma is observed in the OCT images as an excavation of the posterior pole often involving the macular region.[8] This unusual morphological shape is usually found in highly myopic eyes and is very rare in eyes that are not highly myopic.[9]

In our earlier study, we quantitatively analyzed the macular curvature of 143 patients with RP and reported a high incidence of steeper macular curvatures, including staphylomas, even in RP eyes that

are not highly myopic.[10] However, due to the cross-sectional nature of the data collection, the longitudinal changes of the macular curvature were not determined during the course of the retinal degeneration.

Thus, the purpose of this study was to evaluate the longitudinal alterations of the macular curvature of individual eyes with RP and to determine the factors affecting the changes in macular shape.

Materials and Methods

This was a retrospective longitudinal study of 107 RP patients. All of the procedures adhered to the tenets of the Declaration of Helsinki, and the Institutional Review Board/Ethics Committee of Nagoya University Hospital approved the procedures. The Institutional Review Board also waived the need for a written informed consent from the patients because the study design was a retrospective chart review.

Subjects

The medical records of 303 RP patients who were followed by one of the authors (S.U.) at Nagoya University Hospital between March 2013 and December 2017 were reviewed. The diagnosis of RP was based on the presence of night blindness, constriction of the visual fields, attenuation of retinal vessels, bone-spicule retinal pigmentation, and reduced (<100 μV) or extinguished full-field scotopic flash electroretinograms (ERGs) elicited by 300 cd·s/m^2 (PE300; Tomey, Nagoya, Japan). Of the 303 potential patients, we analyzed the right eyes of 107 patients (63 women and 44 men) who had had spectral-domain OCT (SD-OCT; Heidelberg Engineering, Heidelberg, Germany) images obtained at least twice and whose eyes had an axial length (AL) that ranged from 21.5 to 26.0 mm (IOLMaster; Carl Zeiss Meditec, Inc., Dublin, CA). When the axial length was measured several times, the most recent value was used for the statistical analyses. Cross-sectional SD-OCT images of 9-mm horizontal and vertical scans through the center of the fovea were analyzed. The cross-sectional OCT scans were the averages of 100 SD-OCT images that were recorded using the eye-tracking system. The OCT images of two time points—the baseline and a follow-up period that was at least 1 year later—were compared, and when the OCT images were taken more than twice the initial (baseline) and the most recent (follow-up) images were used for the statistical analyses.

Measurement of Retinal Morphological Parameters in SD-OCT Images

The methods to measure the macular curvature in the SD-OCT images have been described in detail.[10] Briefly, each horizontal and vertical SD-OCT image was corrected for the difference in the pixel resolution in the transverse and longitudinal directions. Then, the reflective line corresponding to Bruch's membrane across the fovea (yellow line in Fig. 1A in Ref. 10) was measured quantitatively using MATLAB software (MathWorks, Natick, MA). Eleven to 12 points were marked on the Bruch's membrane line beginning from the center of the fovea, and the marks were separated by 200 pixels (approximately 760 μm) in the SD-OCT images (yellow triangles in Fig. 1A in Ref. 10). The software calculated the approximate curvature of the marked points using a cubic spline interpolation program (yellow and red line in Fig. 1B in Ref. 10). From the calculated curve, a curvature of approximately 6 mm including the central fovea (red line in Fig. 1B in Ref. 10) was selected. The software calculated the mean curvature ±3 mm from the central fovea by using all measured values for the local curvature in 1-μm steps—the mean macular curvature index (MMCI), with units of μm^{-1}. A minus MMCI value indicated a concave shape and a plus values indicated a convex shape.

Ellipsoid Zone Width Measurement

The width of the EZ was measured between the borders where the EZ band met the upper surface of the retinal pigment epithelium by the built-in caliper.[11] If the EZ width exceeded the scanned images, the border of the EZ was set at the edge of the scanned image. All of the measurements were performed using Heidelberg Eye Explorer software (Heidelberg Engineering).

Best-Corrected Visual Acuity

The best-corrected visual acuity (BCVA) was determined on the same day as the recording of the OCT images, and the decimal BCVA was converted to logarithm of the minimum angle of resolution (logMAR) units for statistical analyses. Counting fingers, hand motion, light perception, and no light perception were designated as 1.85, 2.30, 2.80, and 2.90 logMAR units, respectively.[12]

Table. Clinical Data at Baseline and Follow-Up Period

	Baseline	Follow-Up	*P*
BCVA (logMAR)	0.22 ± 0.30	0.29 ± 0.35	<0.001*
Vertical MMCI ($\times 10^{-5}$ μm^{-1})	−15.47 ± 9.52	−16.36 ± 9.78	0.008*
Horizontal MMCI ($\times 10^{-5}$ μm^{-1})	−14.38 ± 9.09	−14.59 ± 9.22	0.36
EZ width of vertical scan (μm)	2158 ± 2136	1883 ± 2100	<0.0001*

*Statistical significance ($P < 0.05$).

Statistical Analyses

Paired *t*-tests were used to determine the significance of the difference of the BCVA and EZ width between the baseline and final examinations. One-sample *t*-tests were used to determine the significance of the differences in the MCCI between the baseline and follow-up period, and whether the ratio of changes in the MMCI was zero or not was analyzed. The ratio of changes in the MMCI (μm^{-1}/day) was calculated by dividing the difference in the MMCI (μm^{-1}) between the baseline and the follow-up period by the time periods (days). Pearson's product–moment correlation tests were used to determine the significance of the correlations between the EZ width and the ratio of changes in the MMCI. $P < 0.05$ was considered to be statistically significant. All statistical analyses were performed using R 3.4.3 (R Foundation for Statistical Computing, Vienna, Austria) and EZR 1.36 software (Saitama Medical Center, Jichi Medical University, Saitama, Japan).

Results

For the RP patients, the mean age ± SD was 45.9 ± 16.2 years at the baseline, with a range of 11 to 85 years. Changes in the OCT images during a mean interval of 3.4 ± 1.4 years were analyzed. The BCVA, MMCI in vertical and horizontal images, and EZ width in the vertical images at the baseline and follow-up periods are summarized in the Table. The mean axial length was 23.80 ± 1.05 mm

Our results showed that the BCVA and the EZ width decreased significantly during the observation period ($P < 0.001$, paired *t*-tests). The MMCI also decreased significantly from –15.47 × 10^{-5} μm^{-1} to –16.36 × 10^{-5} μm^{-1} in the vertical scan images ($P = 0.008$, one-sample *t*-test). This indicated that the shape of the macular became more concave in this plane. In contrast, the MMCI in the horizontal scan did not change significantly ($P = 0.36$, one-sample *t*-test).

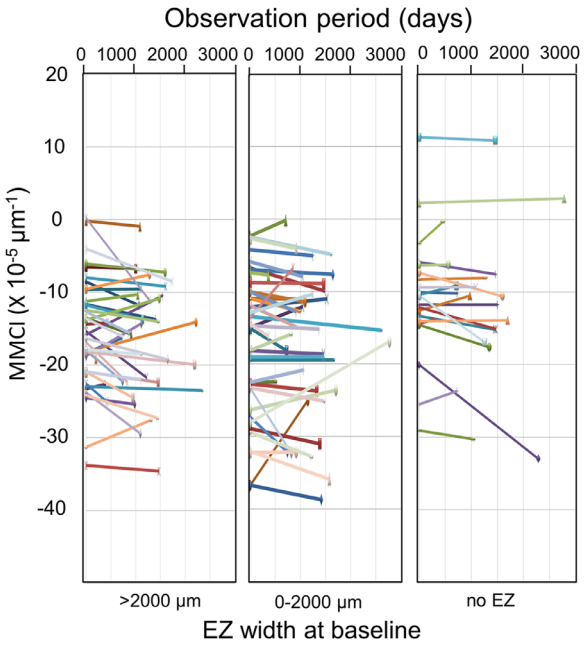

Figure 1. Graphs showing changes in the MMCI (μm^{-1}) in the vertical scan images of all evaluated eyes during the observation period (days). The data were divided into three groups according to the baseline EZ width (>2000 μm, 0–2000 μm, or no EZ).

The changes in the MMCI in the vertical scans of all eyes during the observation period are presented in Figure 1. The MMCI became more concave in 69 eyes and less concave in 38 eyes during the follow-up period. Six eyes had a reduction in the MMCI of more than 5 × 10^{-5} μm^{-1}, and the MMCI increased by more than 5 × 10^{-5} μm^{-1} in four eyes.

Optical Coherence Tomographic Images of Representative Eyes

Figure 2 shows representative OCT images of three eyes for which the MMCI decreased by more than 5 × 10^{-5} μm^{-1} (Figs. 2A–2C) and two eyes for which the MMCI increased by more than 5 × 10^{-5} μm^{-1} (Figs. 2D, 2E). A plot of the changes of the MMCI in these patients is shown at the bottom of Figure 2. The shape of the macula of three eyes (Figs. 2A–2C) became

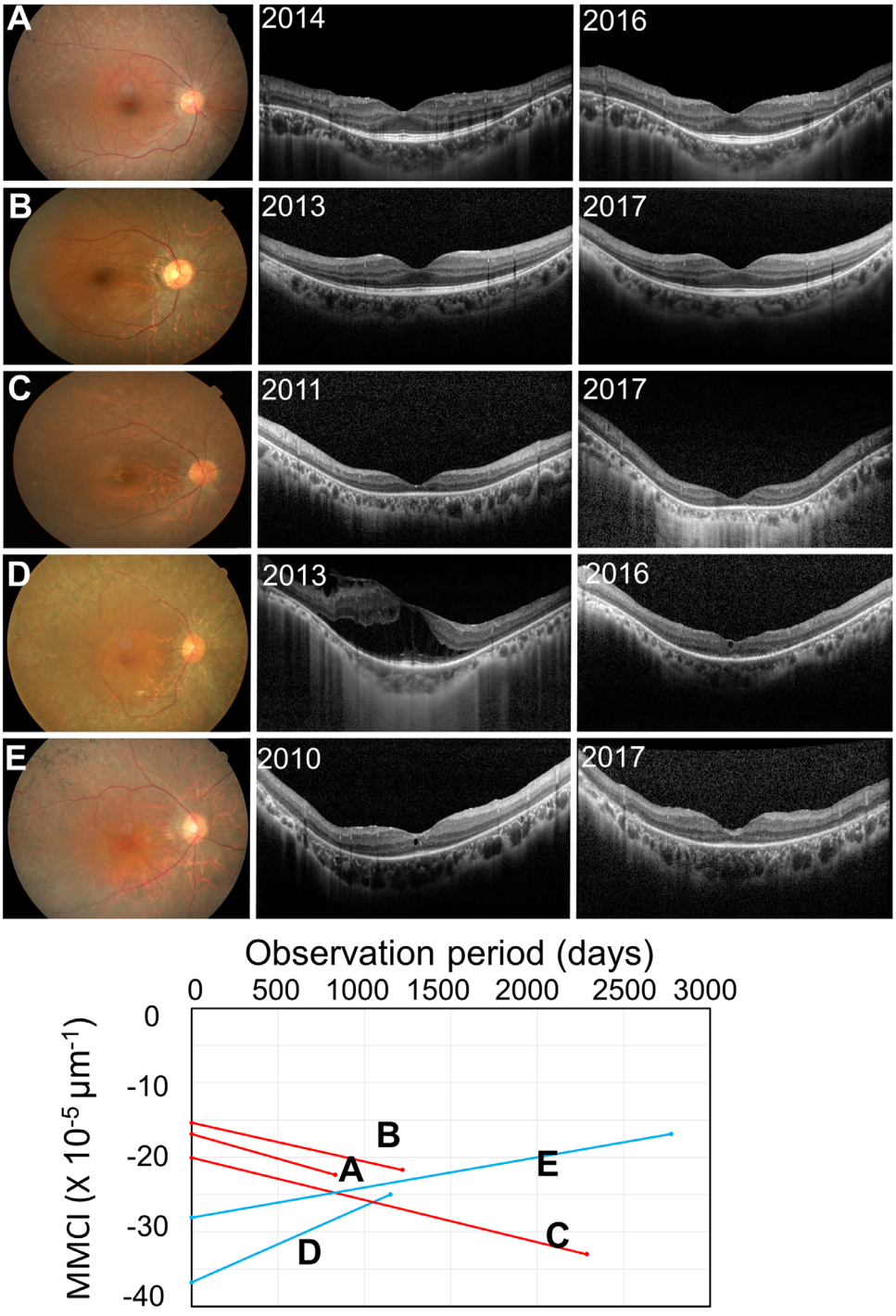

Figure 2. Five representative cases showing large changes in the MMCI during the observation period. Fundus images (*left*) and vertical OCT images at the baseline (*middle*) and at the follow-up period (*right*) of the right eyes of five RP patients are shown at the *top*. The shape of three eyes (A–C) became more concave and the shape of two eyes (D, E) became flatter during the observation periods. Plots of changes in the MMCI (μm^{-1}) for these five representative eyes are shown at the *bottom*. Patient A was a 30-year-old woman with an AL at baseline of 23.54 mm. The MMCI decreased from -16.9×10^{-5} μm^{-1} to -22.3×10^{-5} μm^{-1}, and the width of the EZ was reduced from 4726 µm to 3795 µm in 828 days. Patient B was a 35-year-old woman with an AL at baseline of 24.99 mm. The MMCI decreased from -15.4×10^{-5} μm^{-1} to -21.7×10^{-5} μm^{-1}, and the EZ width was reduced from 6706 µm to 6662 µm in the 1219 days of follow-up period. Patient C was a 29-year-old man with an AL at baseline of 24.31 mm. The MMCI decreased from -20.0×10^{-5} μm^{-1} to -33.0×10^{-5} μm^{-1} in 2285 days, and there was no visible EZ at the baseline. Patient D was a 57-year-old woman with an AL at baseline of 22.39 mm. The MMCI increased from -36.8×10^{-5} μm^{-1} to -25.0×10^{-5} μm^{-1} in 1148 days, and there was no visible EZ at the baseline. The macular edema was absorbed during the observation period. Patient E was a 28-year-old man with an AL at baseline of 24.35 mm. The MMCI increased from -28.1×10^{-5} μm^{-1} to -16.9×10^{-5} μm^{-1}, and EZ width decreased from 956 µm to zero in 2772 days.

steeper despite the variety of changes in the neurosensory retina, preserved middle EZ width (Fig. 2A), long EZ width (Fig. 2B), non-detectable EZ, and thinning of the ONL (Fig. 2C). On the other hand, the MMCIs of two eyes (Figs. 2D, 2E) increased with the absorption of the macular edema. The macular shape became flatter after a resolution of the severe macular edema (Fig. 2D). Among the four eyes for which the MMCI increased more than 5×10^{-5} μm^{-1}, three of the eyes showed a reduction of the macular edema.

Changes in Width of EZ and MMCI

The mean ± SD of the width of the EZ in the vertical OCT images was significantly reduced from 2158 ± 2136 µm at the baseline to 1883 ± 2100 µm ($P < 0.0001$) during the follow-up period (Table). The mean change in the ratio of the MMCI was $8.43 \pm 30.7 \times 10^{-9}$ μm^{-1}/day. The ratio of changes in the MMCI and the baseline width of the EZ were not significant in all eyes ($P = 0.056$, Pearson's product–moment correlation tests) (Fig. 3). This was also true for eyes with visible EZ ($P = 0.125$; $n = 84$). These results indicate that the correlation between the integrity of the retina in patients with RP and changes in the MMCI was not significant. In an earlier study, we found a nonlinear relationship between the EZ width and the MMCI; the MMCI was lower in eyes with an EZ width of around 2200 µm, and the MMCI was higher in eyes with shorter or longer EZ widths.[10] Thus, we divided the eyes into three groups according to the EZ width at the baseline; >2000 µm (mild, 42 eyes), between 0 and 2000 µm (moderate, 42 eyes), and no EZ (severe, 23 eyes). Only the mild group had a significant change in the MMCI during the experimental period ($P = 0.011$, one-sample *t*-test). No significant changes in the MMCI were detected in the moderate cases ($P = 0.474$) or severe cases ($P = 0.148$). We also calculated the correlation between the ratio of changes in the MMCI (μm^{-1}/day) and the ratio of changes in the EZ width (µm/day). Our results showed that there was no significant correlation between the ratio of changes in the MMCI and the ratio of changes in the EZ width ($P = 0.70$, Pearson's product–moment correlation tests; data not shown).

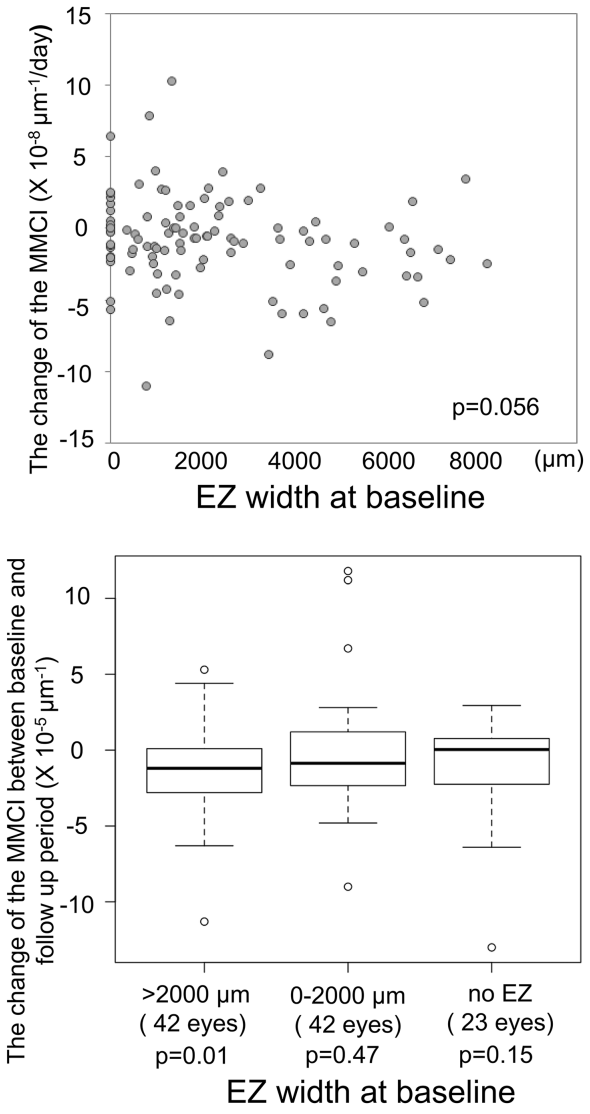

Figure 3. Relationship between the mean ratio of changes in the MMCI (μm^{-1}/day) and the baseline EZ width in the horizontal OCT image in all 107 right eyes with RP (*top*). The correlation between the ratio of changes in the MMCI (μm^{-1}/day) and baseline EZ width ($P = 0.056$, Pearson's product–moment correlation tests, *top*) was not significant. Changes in the MMCI (10^{-5} μm^{-1}) from baseline to the follow-up period for the three groups are shown at the *bottom*. The eyes were divided into three groups according to the length of the EZ width at baseline: >2000 µm (mild, 42 eyes), 0 to 2000 µm (moderate, 42 eyes), or no EZ (severe, 23 eyes). Only the eyes in the mild group had a significant reduction of the MMCI ($P = 0.011$, one–sample *t*-test).

Discussion

Our results showed that the shape of the macular in the vertical OCT image became significantly steeper during a mean of 3.4 years of the experimental period. The eyes with preserved EZ width had a greater change to a steeper macular shape;

however, statistical analysis showed no significant linear correlation of the vertical macular curvature change and the EZ width. This is similar to the findings in our previous study, which found that the MMCI was lowest in eyes with an EZ width of around 2200 µm,

and the MMCI was higher in eyes with shorter or with longer EZ widths.[10]

Combining the results of these two studies, a shorter EZ was associated with a steeper macular curvature in eyes with an EZ width >2000 µm, and the macular curvature was the steepest in eyes with an EZ width of around 2000 µm. However, a further shortening of the EZ did not change the macular curvature.

The shape of the posterior pole is related to the presence of residual photoreceptors and the integrity of the inner retina. Greater increases in the MMCI were found in eyes after the macular edema was absorbed. Macular edema is a common complication associated with RP, and the prevalence of macular edema in RP eyes has been reported to be between 10% and 40%.[13–15] Thus, the shape of the macula in eyes with RP should be affected by the macular edema and its resolution.

Although we found only two factors significantly correlated with the shape of the macula, the degenerating retina does not consistently become steeper, and 36% of the eyes became flatter. These findings indicate that there are probably other factors that are associated with the shape of the macula in RP eyes.

One of these factors may be the structure of the choroid. Thin choroids are usually associated with staphylomas in highly myopic eyes, and reduced choroidal thickness has been reported in RP eyes.[16] The thinning of the choroid might be the cause of the steeper macular shape in eyes with RP. OCT performed with enhanced depth imaging would be useful for analyzing the relationship between choroidal thickness and macular shape in future studies.

Another factor that could affect the shape of the macula might be structural changes of the inner retina caused by retinal remodeling.[17–19] Although RP is initially a disorder of the photoreceptors, the inner retina has been reported to become progressively disorganized with a reprogramming of the retinal bipolar cells, alterations in protein signatures of the neurons, and intense gliosis of the Müller glial cells.[20] It is difficult to analyze the retinal remodeling from the OCT images; however, it is important to understand that the effects of changes of the inner retina on macular shape should be considered in RP eyes.

There were significant changes of the vertical macular curvature but no significant changes in the horizontal macular curvature. It is known that in highly myopic eyes the speed of development of staphyloma is different among the sites of the retina; the superior and temporal retina are more easily affected.[21] Thus, the ratio of the changes of the macular curvature might differ between the horizontal and vertical axes. Actually, the MMCI of the horizontal axis (-14.03×10^{-5} µm^{-1}) was higher than that of vertical axis (-15.47×10^{-5} µm^{-1}). The horizontal axis may be less flexible than the vertical axis because the optic disc is connected to the eye; the optic disc is fixed to the optic nerve canal, preventing stretching of the sclera and choroid. In our previous study, the high incidence of steeper macular curvatures in the horizontal axis in RP eyes compared with that of normal control eyes (-6.63×10^{-5} µm^{-1}) was reported.[10] Macular curvature in the horizontal axis appears to change too slowly to have been detected during the observation period of this study.

There are several limitations in this study. The formation of a posterior staphyloma has been reported to be associated with early-onset retinal dystrophy[5,22–25]; however, we included only patients older than 10 years of age, and progression of the steep macular curvature in earlier onset RP cases, including Leber congenital amaurosis, might differ. Second, we did not analyze the genotype–phenotype correlations because of the lack of patients who were identified by causative gene variants. Analyses of the associated genes and changes of the macular curvatures might provide further information on the formation of the steep macular curvature in RP eyes. Third, the axial length is a key factor in the formation of a staphyloma; however, we did not follow the changes of the axial length, so we could not evaluate the influence of changes in axial length on the formation of steep macular curvature in our cohort. Fourth, the observation period was too short to determine the factors influencing changes in the MMCI. It would be necessary to evaluate changes in the MMCI periodically for a long time into the future.

In conclusion, we detected a progressive development of a steeper macular curvature in RP eyes with increasing time. In addition, the integrity of the EZ and resolution of the macular edema were related to changes of the macular shape. Progression of the concave shape of the macula in RP should be considered with regard to implantation of retinal prostheses, because signal transduction from the electrodes to retinal target cells appears to be inhibited by an excessive electrode–retina distance.[6]

Further studies on the importance of the concave shape of the macular in RP eyes should be conducted; for example, does the steep curvature protect or accelerate retinal degeneration?

Acknowledgments

The authors thank Duco Hamasaki, PhD (Bascom Palmer Eye Institute), for the discussions and editing

the final version of the manuscript. This research was conducted on behalf of the Joint PhD program between Nagoya University and Lund University.

Supported in part by KAKENHI Grants from the Japan Society for the Promotion of Science (19K09928 to S.U; 16K11265 to Y.I.).

Disclosure: **M. Meinert**, None; **S. Ueno**, None; **S. Komori**, None; **Y. Koyanagi**, None; **A. Sayo**, None; **S. Andreasson**, None; **T. Kominami**, None; **Y. Ito**, None; **H. Terasaki**, None

References

1. Fischer MD, Fleischhauer JC, Gillies MC, Sutter FK, Helbig H, Barthelmes D. A new method to monitor visual field defects caused by photoreceptor degeneration by quantitative optical coherence tomography. *Invest Ophthalmol Vis Sci*. 2008;49:3617–3621.
2. Jacobson SG, Aleman TS, Sumaroka A, et al. Disease boundaries in the retina of patients with Usher syndrome caused by MYO7A gene mutations. *Invest Ophthalmol Vis Sci*. 2009;50:1886–1894.
3. Hood DC, Ramachandran R, Holopigian K, Lazow M, Birch DG, Greenstein VC. Method for deriving visual field boundaries from OCT scans of patients with retinitis pigmentosa. *Biomed Opt Express*. 2011;2:1106–1114.
4. Birch DG, Locke KG, Felius J, et al. Rates of decline in regions of the visual field defined by frequency-domain optical coherence tomography in patients with RPGR-mediated X-linked retinitis pigmentosa. *Ophthalmology*. 2015;122:833–839.
5. Kuniyoshi K, Sakuramoto H, Yoshitake K, et al. Longitudinal clinical course of three Japanese patients with Leber congenital amaurosis/early-onset retinal dystrophy with RDH12 mutation. *Doc Ophthalmol*. 2014;128:219–228.
6. Parmeggiani F, De Nadai K, Piovan A, Binotto A, Zamengo S, Chizzolini M. Optical coherence tomography imaging in the management of the Argus II retinal prosthesis system. *Eur J Ophthalmol*. 2017;27:e16–e21.
7. Xu X, Fang Y, Yokoi T, et al. Posterior staphylomas in eyes with retinitis pigmentosa without high myopia. *Retina*. 2019;39:1299–1304.
8. Ohno-Matui K. Staphyloma. In: Spaide RF, Ohno-Matsui K, Yannuzzi LA, eds. *Pathologic Myopia*. New York, NY: Springer; 2014:167–176.
9. Numa S, Yamashiro K, Wakazono T, et al. Prevalence of posterior staphyloma and factors associated with its shape in the Japanese population. *Sci Rep*. 2018;8:4594.
10. Komori S, Ueno S, Ito Y, et al. Steeper macular curvature in eyes with non-highly myopic retinitis pigmentosa. *Invest Ophthalmol Vis Sci*. 2019;60:3135–3141.
11. Kominami T, Ueno S, Kominami A, et al. Associations between outer retinal structures and focal macular electroretinograms in patients with retinitis pigmentosa. *Invest Ophthalmol Vis Sci*. 2017;58:5122–5128.
12. Schulze-Bonsel K, Feltgen N, Burau H, Hansen L, Bach M. Visual acuities "hand motion" and "counting fingers" can be quantified with the Freiburg visual acuity test. *Invest Ophthalmol Vis Sci*. 2006;47:1236–1240.
13. Fishman GA, Gilbert LD, Anderson RJ, Marmor MF, Weleber RG, Viana MAG. Effect of methazolamide on chronic macular edema in patients with retinitis-pigmentosa. *Ophthalmology*. 1994;101:687–693.
14. Hajali M, Fishman GA, Anderson RJ. The prevalence of cystoid macular oedema in retinitis pigmentosa patients determined by optical coherence tomography. *Br J Ophthalmol*. 2008;92:1065–1068.
15. Hirakawa H, Iijima H, Gohdo T, Tsukahara S. Optical coherence tomography of cystoid macular edema associated with retinitis pigmentosa. *Am J Ophthalmol*. 1999;128:185–191.
16. Dhoot DS, Huo S, Yuan A, et al. Evaluation of choroidal thickness in retinitis pigmentosa using enhanced depth imaging optical coherence tomography. *Br J Ophthalmol*. 2013;97:66–69.
17. Jones BW, Kondo M, Terasaki H, Lin Y, McCall M, Marc RE. Retinal remodeling. *Jpn J Ophthalmol*. 2012;56:289–306.
18. Okado S, Ueno S, Kominami T, et al. Temporal properties of flicker ERGs in rabbit model of retinitis pigmentosa. *Invest Ophthalmol Vis Sci*. 2017;58:5518–5525.
19. Ueno S, Kominami T, Okado S, Inooka D, Kondo M, Terasaki H. Course of loss of photoreceptor function and progressive Müller cell gliosis in rhodopsin P347L transgenic rabbits. *Exp Eye Res*. 2019;184:192–200.
20. Jones BW, Pfeiffer RL, Ferrell WD, Watt CB, Marmor M, Marc RE. Retinal remodeling in human retinitis pigmentosa. *Exp Eye Res*. 2016;150:149–165.
21. Takahashi A, Ito Y, Iguchi Y, Yasuma TR, Ishikawa K, Terasaki H. Axial length increases and related changes in highly myopic normal eyes with myopic complications in fellow eyes. *Retina*. 2012;32:127–133.

22. Koenekoop RK, Wang H, Majewski J, et al. Mutations in NMNAT1 cause Leber congenital amaurosis and identify a new disease pathway for retinal degeneration. *Nat Genet*. 2012;44:1035–1039.
23. Khan AO, Eisenberger T, Nagel-Wolfrum K, Wolfrum U, Bolz HJ. C21orf2 is mutated in recessive early-onset retinal dystrophy with macular staphyloma and encodes a protein that localises to the photoreceptor primary cilium. *Br J Ophthalmol*. 2015;99:1725–1731.
24. Ajmal M, Khan MI, Neveling K, et al. A missense mutation in the splicing factor gene *DHX38* is associated with early-onset retinitis pigmentosa with macular coloboma. *J Med Genet*. 2014;51:444–448.
25. Pierrache LHM, Kimchi A, Ratnapriya R, et al. Whole-exome sequencing identifies biallelic IDH3A variants as a cause of retinitis pigmentosa accompanied by pseudocoloboma. *Ophthalmology*. 2017;124:992–1003.